Low-Temperature Magnets $M[N(CN)_2]_2$(pyrimidine) (M = Fe and Co) with a 3-D Network

Takaharu Kusaka, Takayuki Ishida,* Daisuke Hashizume, Fujiko Iwasaki, and Takashi Nogami*
The University of Electro-Communications, Chofu, Tokyo 182-8585

(Received July 10, 2000 ; CL-000654)

X-Ray crystal structure analyses reveal that the title complexes have a 3-D network, in which $N(CN)_2^-$ and pyrimidine contribute μ-1,5-bridged 2-D and μ-1,3-bridged 1-D structures, respectively. Magnetic measurements indicate that the Fe and Co complexes have spontaneous magnetizations below the transition temperatures of 3.2 and 1.8 K, respectively.

There have been numerous reports in which N-donor bridging ligands have been used to form infinite metal-organic polymeric frameworks.[1] We have reported the magnetism of pyrimidine-bridged transition metal complexes in connection with the high-spin *m*-phenylene-bridged poly-carbenes and -radicals.[2] Various magnets have also been reported containing d-transition metal ions and polycyano-anion bridges such as $N(CN)_2^-$ [3] and $C(CN)_3^-$.[4] Ternary systems are of increasing interest, and the peculiar crystal structures have been reported for $Mn[N(CN)_2]_2(pz)$,[5] $Cu[N(CN)_2]_2(pz)$,[6] and $Ag[C(CN)_3](pz)$[7] (pz = pyrazine). We report here the crystal structure and magnetic phase transition of $M^{II}[N(CN)_2]_2(pm)$ [M = Fe (**1**), Co (**2**); pm = pyrimidine) containing both $N(CN)_2^-$ and pm bridges.

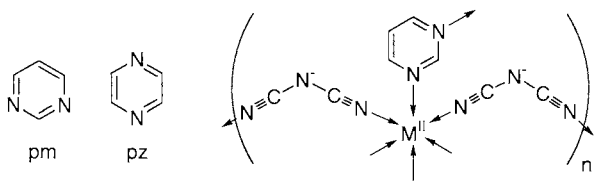

1: M = Fe, **2**: M = Co

An EtOH–H_2O solution containing pm and $NaN(CN)_2$ with a 1/2 molar ratio was added to an aqueous solution of $FeCl_2 \cdot 4H_2O$ which was equimolar of pm. The mixture was allowed to stand for several days to give yellow single crystals of **1**. A similar procedure using $CoCl_2 \cdot 6H_2O$ in place of $FeCl_2 \cdot 4H_2O$ gave red crystals of **2**. Elemental analysis indicates that the crystals contain 0.5–1.0 molar of EtOH as a crystal solvent. X-Ray diffraction data were collected on a Rigaku Raxis-Rapid IP diffractometer with monochromated Mo Kα radiation. Magnetic properties were measured on Quantum Design MPMS SQUID and PPMS ac/dc magnetometers equipped with 7 and 9 T superconducting magnets, respectively.

The X-ray crystal structure analysis[8] of **1** reveals that Fe^{II} and $N(CN)_2^-$ ions construct a two-dimensional network parallel to the *ac*-plane and that pm molecules bridge inter-sheet Fe^{II} ions (Figure 1). Along the *b*-axis, Fe ions and pm bridges form a *trans* zigzag chain. Each octahedral Fe ion resides at an inversion center and is coordinated by four nitrile nitrogen atoms at the equatorial sites with the Fe–N distances of 2.138(4) and 2.142(4) Å, and by two pm nitrogen atoms at the axial sites with the Fe–N distance of 2.202(4) Å. The N(nitrile)–Fe–N(pm) angles range from 89.6(2) to 90.4(2)°.

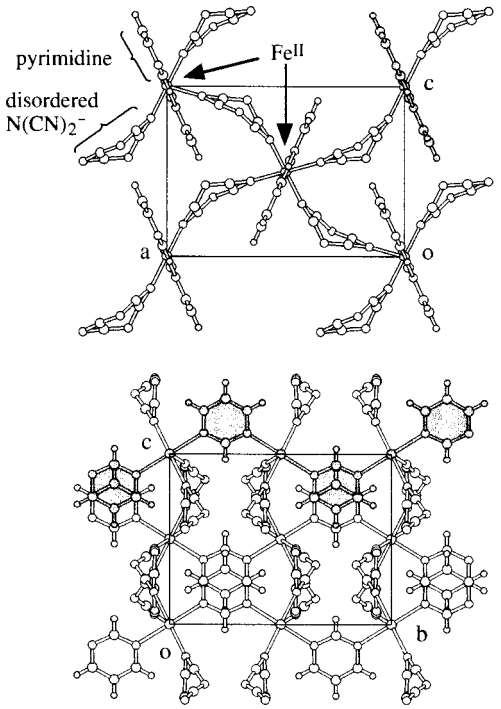

Figure 1. Crystal structure of $Fe[N(CN)_2]_2(pm)$ (**1**), viewed along the *b* (top) and *a* axes (bottom). Disordered solvent molecules are omitted for the sake of clarity. A one-dimensional Fe-pm chain is shaded.

The intra-sheet Fe···Fe separation is 7.9458(5) Å across the NCNCN atoms. The amide nitrogen atom does not act as an N-donor. The $N(CN)_2^-$ moiety was disordered into two positions. The central C–N–C angles are 119(1) and 121(1)°, the N–C≡N angles 173(2)–176(1)°, and the C≡N–Fe angles 153.8(8)–171(1)°. The Fe···Fe separation of 6.0220(3) Å across the pm bridge is shorter than that across the $N(CN)_2^-$ bridge. The pm bridge may afford a principal magnetic exchange pathway. Due to the strong directionality of the pm lone-pairs, the elongated octahedral axes of neighboring Fe ions are relatively canted by 112.0(2)°.

The X-ray crystallographic analysis of **2**[9] revealed that the crystal of **2** was isomorphous to that of **1**. The Co–N bond lengths are 2.103(4) and 2.105(4) Å for nitrile nitrogen atoms and 2.154(4) Å for pm nitrogen atoms.

Figure 2(a) shows the temperature dependence of the product of magnetic susceptibility and temperature ($\chi_{mol}T$) for **1** and **2** measured at 5 kOe. As a decrease of temperature, the $\chi_{mol}T$ value decreased down to ca. 8 K, but turned to increase to exhibit a peak at 3.6 K. Below 3.6 K, the $\chi_{mol}T$ value decreased again, which is mainly due to a saturation effect as described below. Above 8 K, a fit to the Curie–Weiss equation with a temperature-independent paramagnetism [$\chi_{mol} = C/(T - \theta) + N\alpha$] gave C = 4.40 cm^3 K mol^{-1}, θ = –7.0 K, and $N\alpha = 2.4 \times 10^{-2}$

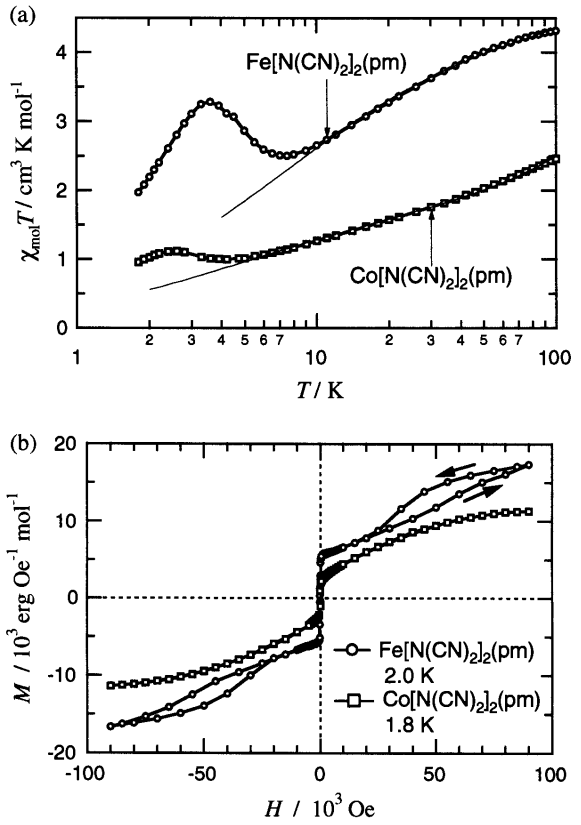

Figure 2. a) Temperature dependence of the product $\chi_{mol}T$ for **1** (circles) and **2** (squares) measured at 5 kOe. The solid lines represent calculated Curie-Weiss behavior. For the parameters, see the text. b) Magnetization curves of **1** (circles) and **2** (squares) measured at 2.0 and 1.8 K, respectively.

cm^3 mol^{-1} as shown with a solid line in Figure 2(a).[10] These values clearly indicate the presence of antiferromagnetic interaction among the Fe^{II} $S = 2$ spins.

The field-cooled magnetization of **1** at 5 Oe exhibited an upsurge around 3.5 K and saturated below 3.3 K. The remnant magnetization disappeared at 3.2 K on heating. The zero-field-cooled magnetization showed a broad maximum at 3.3 K. The ac magnetic susceptibility (χ_{ac}) measurement (10 kHz, 10 Oe) of **1** showed a sharp peak at 3.2 K, which is defined as a magnetic phase transition temperature.

The magnetization curve of **1** measured at 2.0 K exhibited a spontaneous magnetization of 5.8×10^3 erg Oe^{-1} mol^{-1} [Figure 2(b)]. The coercive field was < 20 Oe, indicating a soft character of **1**. Very interestingly, the magnetization started again to increase at ca. 40 kOe and seems to reach a saturation value of $S = 2$ above 90 kOe. A hysteresis could be found on decreasing the magnetic field, demonstrating the bulk ferromagnetism of **1** in this region.

The Curie–Weiss analysis of the magnetism of **2** gave C = 1.73 cm^3 K mol^{-1}, $\theta = -4.4$ K, and $N\alpha = 8.4 \times 10^{-2}$ cm^3 mol^{-1} [Figure 2(a)],[10] indicating the antiferromagnetic interaction among the Co^{II} $S = 3/2$ spins. A very small peak was found at 2.6 K. The χ_{ac} measurement (10 kHz, 10 Oe) of **2** in the absence of any applied dc field showed only a sharp upsurge near the lowest temperature attained (1.8 K), but a peak appeared at 1.9 K when a dc field of 100 Oe was applied. The transition temperature of **2** was estimated to be 1.8 K. The magnetization curve measured at 1.8 K indicated a spontaneous magnetization of 2.5×10^3 erg Oe^{-1} mol^{-1} [Figure 2(b)]. The coercive field was < 20 Oe.

In contrast to antiferromagnetism of $Mn[N(CN)_2]_2(pz)$ containing similar μ-1,5-$N(CN)_2^-$ bridges,[5] **1** and **2** show spontaneous magnetization below their transition temperatures. In view of the presence of antiferromagnetic interactions in **1** and **2**, these magnets are characterized as spin-canted antiferromagnets (weak ferromagnets) like $M^{II}[N(CN)_2]_2$ (M = Fe,[3b] Mn,[3b] and Co[3c]). The magnetization curve of **1** can be explained in terms of metamagnetic transition from a spin-canted antiferromagnet to a ferromagnet. Assuming that these complexes have a pseudo-1-dimensional magnetic structure, inter-chain magnetic interactions may be observed in a low-field region in Figure 2(b). However, we found no anomaly so far except for behavior typical of a weak ferromagnet. Further physical investigation is now in progress.

This work was supported by Grants-in-Aid for Scientific Research (401/11136212, 730/11224204, and 297/12020219) from the Ministry of Education, Science, Sports and Culture, Japan.

References and Notes

1 P. J. Stang and B. Olenyuk, *Acc. Chem. Res.*, **30**, 502 (1997); O. M. Yaghi, H. Li, C. Davis, D. Richardson, and T. L. Groy, *Acc. Chem. Res.*, **31**, 474 (1998).

2 T. Ishida and T. Nogami, *Recent Res. Devel. Pure Appl. Chem.*, **1**, 1 (1997); T. Ishida, K. Nakayama, M. Nakagawa, W. Sato, Y. Ishikawa, M. Yasui, F. Iwasaki, and T. Nogami, *Synth. Met.*, **85**, 1655 (1997); K. Nakayama, T. Ishida, R. Takayama, D. Hashizume, M. Yasui, F. Iwasaki, and T. Nogami, *Chem. Lett.*, **1998**, 497.

3 a) S. R. Batten, P. Jensen, B. Moubaraki, K. S. Murray, and R. Robson, *Chem. Commun.*, **1998**, 439. b) M. Kurmoo and C. J. Kepert, *New J. Chem.*, **22**, 1515 (1998). c) J. L. Manson, C. R. Kmety, Q. Z. Huang, J. W. Lynn, G. M. Bendele, S. Pagola, P. W. Stephens, L. M. Liable-Sands, A. L. Rheingold, A. J. Epstein, and J. S. Miller, *Chem. Mater.*, **10**, 2552 (1998). d) J. L. Manson, C. R. Kmety, A. J. Epstein, and J. S. Miller, *Inorg. Chem.*, **38**, 2552 (1999).

4 S. R. Batten, B. F. Hoskins, B. Moubaraki, K. S. Murray, and R. Robson, *J. Chem. Soc., Dalton Trans.*, **1999**, 2977; H. Hoshino, K. Iida, T. Kawamoto, and T. Mori, *Inorg. Chem.*, **38**, 4229 (1999); J. L. Manson, C. Campana, and J. S. Miller, *Chem. Commun.*, **1998**, 251.

5 J. L. Manson, C. D. Incarvito, A. L. Rheingold, and J. S. Miller, *J. Chem. Soc., Dalton Trans.*, **1998**, 3705.

6 S. R. Batten, B. F. Hoskins, and R. Robson, *New J. Chem.*, **1998**, 173.

7 P. Jensen, S. R. Batten, G. D. Fallon, D. C. R. Hockless, B. Moubaraki, K. S. Murry, and R. Robson, *J. Solid State Chem.*, **145**, 387 (1999).

8 Crystallographic data of **1**•EtOH are: orthorhombic, *Pnma*, a = 12.917(1), b = 12.0440(6), c = 9.2575(8) Å, V = 1440.2(2) $Å^3$, Z = 4, D_{calc} = 1.449 g cm^{-3}, T = 100 K, R = 0.059 [$I > 2\sigma(I)$], and 1663 independent reflections. All the independent reflections were used for the structure refinement. The EtOH moiety is disordered and the atomic displacement parameters are significantly greater than those of the other moieties, indicating smaller occupancy of the EtOH moiety than unity.

9 Crystallographic data of **2**•EtOH are: orthorhombic, *Pnma*, a = 12.8586(4), b = 11.9268(4), c = 9.2126(2) Å, V = 1412.86(7) $Å^3$, Z = 4, D_{calc} = 1.491 g cm^{-3}, T = 100 K, R = 0.067 [$I > 2\sigma(I)$], and 1699 independent reflections. All the independent reflections were used for the structure refinement. The occupancy of EtOH moiety is smaller than unity similarly to the case of **1**•EtOH. See ref. 8.

10 Analysis is based on the molecular formula $M^{II}[N(CN)_2]_2(pm)$.